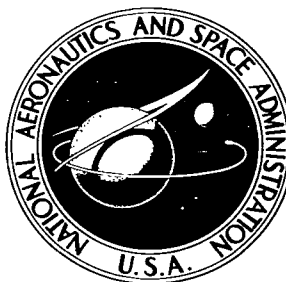


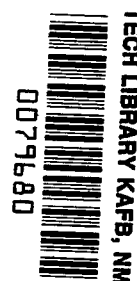
NASA TECHNICAL NOTE



NASA TN D-2768

e. 1

NASA TN D-2768



# THE TERNARY SYSTEM TANTALUM-HAFNIUM-CARBON AT 2050° C

*by Daniel L. Deadmore and Isidor Zaplatynsky*

*Lewis Research Center*

*Cleveland, Ohio*

TECH LIBRARY KAFB, NM



0079680

NASA TN D-2768

# THE TERNARY SYSTEM TANTALUM-HAFNIUM-CARBON AT 2050° C

By Daniel L. Deadmore and Isidor Zaplatynsky

Lewis Research Center  
Cleveland, Ohio

NATIONAL AERONAUTICS AND SPACE ADMINISTRATION

---

For sale by the Clearinghouse for Federal Scientific and Technical Information  
Springfield, Virginia 22151 – Price \$1.00

# THE TERNARY SYSTEM TANTALUM-HAFNIUM-CARBON AT 2050° C

by Daniel L. Deadmore and Isidor Zaplatynsky

Lewis Research Center

## SUMMARY

An isothermal cross section of the tantalum-hafnium-carbon (Ta-Hf-C) system at 2050° C was constructed from x-ray diffraction, chemical analysis, metallographic, and microhardness data. No phases other than those appearing in the three binary systems were observed in the ternary system. A liquid phase was found in a large portion of the hafnium-rich corner of the ternary section.

## INTRODUCTION

The melting points of tantalum carbide (TaC) and hafnium carbide (HfC) are very high ( $\approx 3950^\circ$  and  $3900^\circ$  C, respectively) and the 4-tantalum-carbide - hafnium-carbide ( $4 \text{ TaC} \cdot \text{HfC}$ ) solid solution is a material of the highest known melting point ( $\approx 4100^\circ$  C)(ref. 1). Therefore, compositions within the TaC-HfC pseudobinary system are considered for possible application in the field of high-temperature thermionic energy conversion. In this connection vaporization studies have been conducted (ref. 2) in order to establish the thermal stability of TaC-HfC solid solutions. In the course of that investigation it was observed that compositional changes occurred on the surface of these carbides due to differences in the vaporization rates of tantalum (Ta), hafnium (Hf), and carbon (C). Consequently, a need became apparent for the knowledge of ternary equilibrium phase relations. An experimental study was initiated to determine the ternary diagram at 2050° C. This temperature was chosen because it is within the range of possible thermionic emitter operation. While the present work was in progress, an isothermal section of this system at 1850° C was reported (ref. 3).

Previous literature related to the present work includes binary diagrams for Ta-C (ref. 4), Hf-C (ref. 5), Ta-Hf (ref. 6), and ternary phase relations of Ta-Hf-C at 1850° C (ref. 3). These are shown in figure 1.

In the investigation reported here, the isothermal section at 2050° C of the Ta-Hf-C system was determined. Samples were prepared by several powder-metallurgical techniques and by arc melting. After homogenization heat treatment at 2050° C in vacuum, samples were rapidly cooled, and phase identification was made by x-ray diffraction, metallographic, and microhardness techniques.

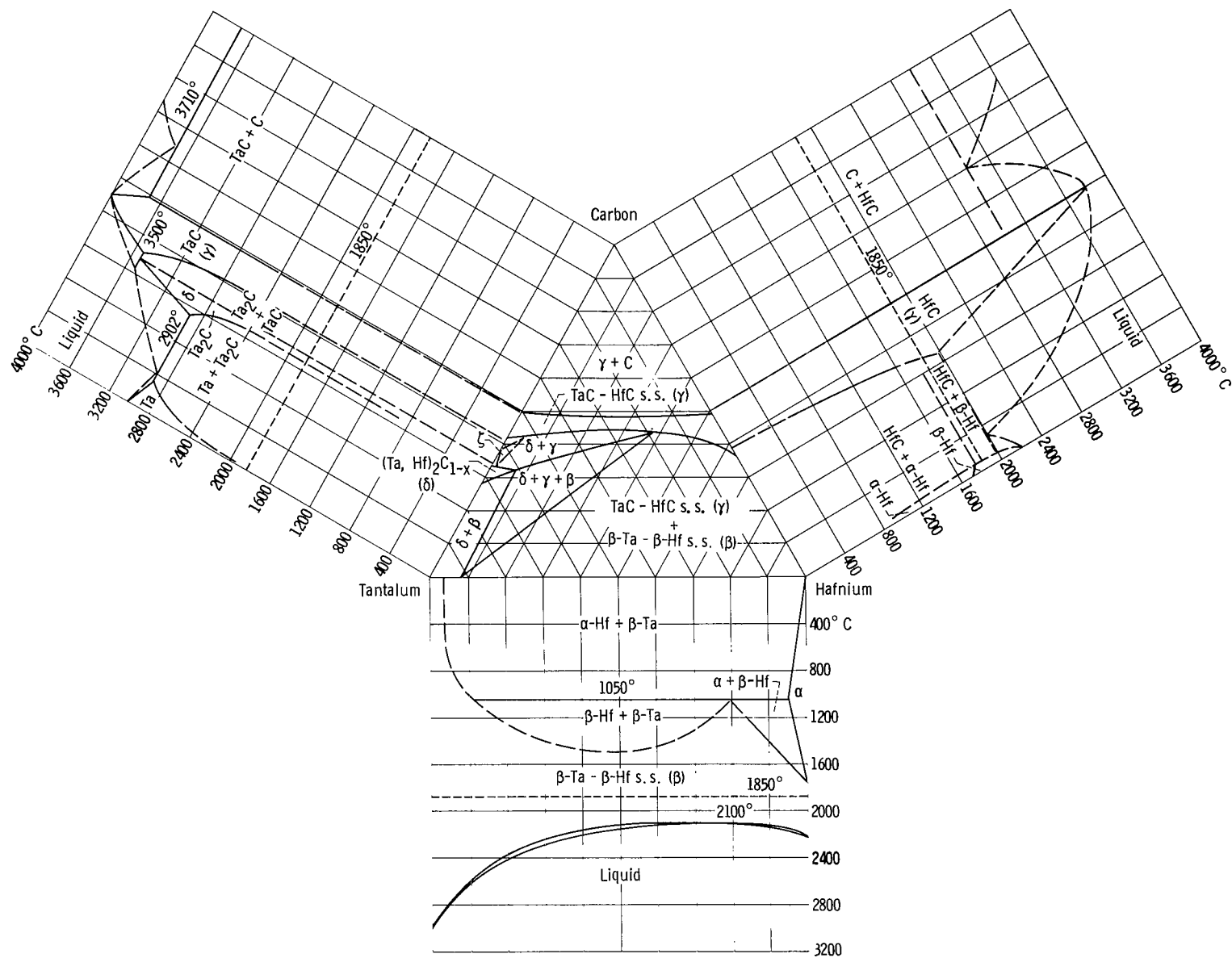


Figure 1. - Binary and ternary tantalum-hafnium-carbon systems given in literature. Ternary system is isothermal section at 1850° C.

## EXPERIMENTAL PROCEDURE

### Sample Preparation

The starting materials used in the preparation of the samples were tantalum hydride (TaH), hafnium-hydride (HfH<sub>2</sub>), and spectrographic grade carbon. The analyses of the hydrides are given in table I.

Samples were prepared by three techniques: (1) sintering of cold-pressed mixtures, (2) hot pressing, and (3) sintering followed by arc melting. The cold-pressed and sintered specimens were prepared by blending the required amounts of the component powders followed by hydrostatically compacting (85 000 psi) at room temperature without a binder. These compacts, contained within thorium oxide crucibles, were set inside a tungsten susceptor and were slowly heated by induction in a vacuum of  $5 \times 10^{-6}$  to  $9 \times 10^{-6}$  torr to avoid rapid evolution of hydrogen. The specimens were brought up to 2050° C and held at that temperature for periods of from 1 to 30 hours until reaction was complete. The specimens were then cooled at a rate of 1000° C per minute to 900° C then more slowly to room temperature. The extent of reaction was determined by x-ray diffraction examination after each 1 to 5 hours of heating. Completion of reaction was assumed when the diffraction pattern showed no change. Several samples were checked for thorium content with an alpha counter. No thorium pickup was indicated.

Some compositions in the pseudobinary TaC-HfC region (about 50 atomic percent C) were hot pressed in graphite dies at 2400° to 2700° C at 3200 pounds per square inch for 1/2 to 1 hour.

Selected compositions were arc melted in argon using a nonconsumable tungsten electrode and a water-cooled copper hearth. The pickup of tungsten by the samples determined by chemical analysis was 0.01 to 0.1 weight percent.

All the hot-pressed and arc-melted samples were heat treated at 2050° C in vacuum for times up to 30 hours and cooled at a rate of 1000° C per minute to 900° C then more slowly to room temperature. This cooling rate is believed to be sufficiently rapid to retain the high-temperature phases except in hafnium-rich compositions where the precipitation of  $\alpha$ -hafnium was observed. Even considerably faster cooling of composition 86 did not arrest the formation of  $\alpha$ -hafnium. All sample compositions, along with phases present at room temperature, are given in table II.

It was also observed that sintered compositions 83, 85, 86, 87, 88 and 89, in the hafnium-rich corner of the diagram, showed large shrinkages, some deformation, and greatly increased densities. These observations suggest the presence of a liquid phase at 2050° C.

### Measurements

Since it was expected that carbon loss would occur during preparation and heat treatment, all final products were analyzed for total and free carbon and the final composition calculated accordingly.

Temperature determinations were made with a disappearing-filament-type micro-optical pyrometer calibrated against a standard tungsten strip lamp (including the optical prism, which was part of the furnace). Temperature was determined with an accuracy of  $\pm 30^{\circ}$  C.

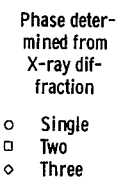
A room-temperature x-ray diffraction study was done on powdered samples (taken from the center of the specimens) with nickel-filtered copper radiation using a diffractometer. In the case of metal-phase-rich compositions, which could not be easily ground, the patterns were taken from the interior cross section of the specimen. The lines on each pattern were indexed without difficulty because the structures of the phases involved were cubic or hexagonal. Lattice parameters were calculated on a 7094 computer by the least-squares method using the  $1/\sin^2\theta$  extrapolation function. The standard deviation of all lattice parameters was  $\pm 0.005$  angstrom.

All arc-melted and some of the sintered compositions were examined by a metallographic technique. Etching was done with a mixture of hydrofluoric acid, nitric acid, and water. The composition of the etchant varied from one sample to another. When possible, the Knoop microhardness of the phases was determined with a 50-gram load. The hardness numbers reported are the average of 15 indentations. The standard deviation is  $\pm 10$  percent of the reported value.

## RESULTS

### X-ray Diffraction Study

The examination of the x-ray patterns revealed that no phases were present other than those appearing in the three binary systems. These are the face-centered-cubic  $\gamma(\text{Ta,Hf})\text{C}_{1-x}$ , hexagonal  $\delta(\text{Ta,Hf})_2\text{C}_{1-x}$ , hexagonal  $\alpha(\text{Hf,Ta})$ , and body-centered-cubic  $\beta(\text{Ta,Hf})$  phases. Of course, the lattice parameters of these phases changed with the composition. This change was particularly large in the case of the TaC-HfC solid solution. The number and identity of the phases in each composition were determined as shown in figure 2. Each composition is identified by its sample number (composition). The same information is tabulated in table II, where, in addition to the number and identity of the phases, the lattice parameters are listed. Since x-ray diffraction patterns were taken at room temperature, the Ta-Hf body-centered-cubic solid solutions in the hafnium-rich corner were in some cases not observed, but instead body-centered-cubic tantalum and the hexagonal form of hafnium were detected. However, it is known from the binary Ta-Hf system that at  $2050^{\circ}$  C there is only one phase present, the  $\beta(\text{Ta,Hf})$  body-centered-cubic solid solution. In some instances when a phase was detected, but there were not enough diffraction lines for accurate determination of the lattice parameter, only its presence was indicated (table II). Since TaC-HfC solid solutions are of considerable practical interest because of their high melting points, their lattice parameters are shown as a function of composition in figure 3. The iso-lattice parameter lines are also drawn with the aid of data taken from references 3, 7, and 8.



5

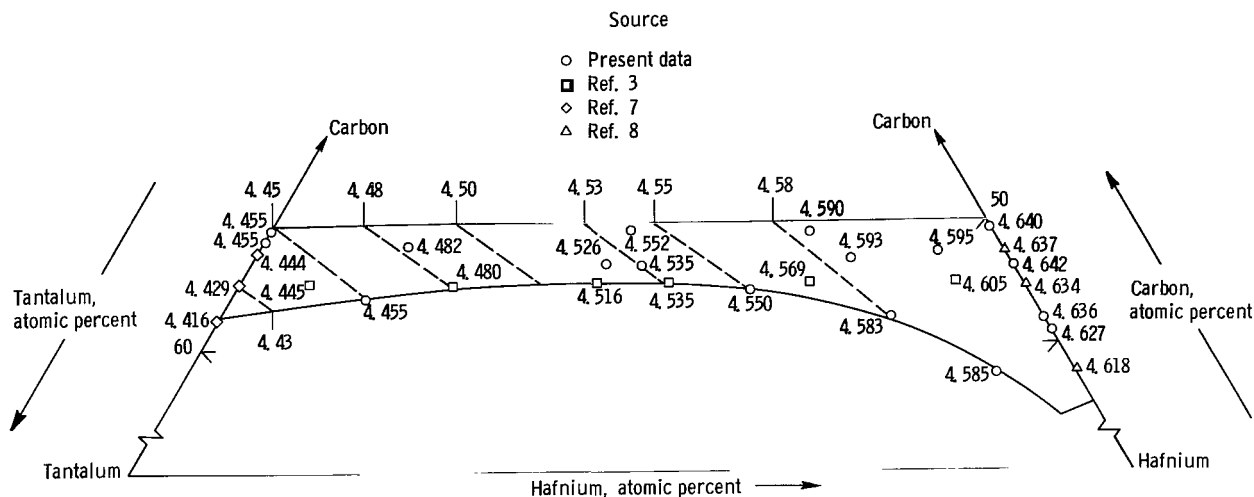


Figure 3. - Lattice parameters in face-centered-cubic ( $\gamma$ ) single-phase region of tantalum-hafnium-carbon system.

### Metallography

The sintered samples containing only small amounts of metallic phase were porous and could not be prepared for metallographic examination. The sintered samples, which contained a significant amount of metallic phase, and the samples which were arc melted, were mounted and polished with diamond compound.

There is agreement between results obtained from metallography and x-ray investigation concerning the number of phases present in a given sample. Representative microstructures of sintered and arc-melted samples are shown in figure 4. The numbers in parentheses indicate the content of Ta, Hf, and C, respectively, in atomic percent. The phases are labeled and their microhardness (Knoop Hardness Number (KHN)) noted.

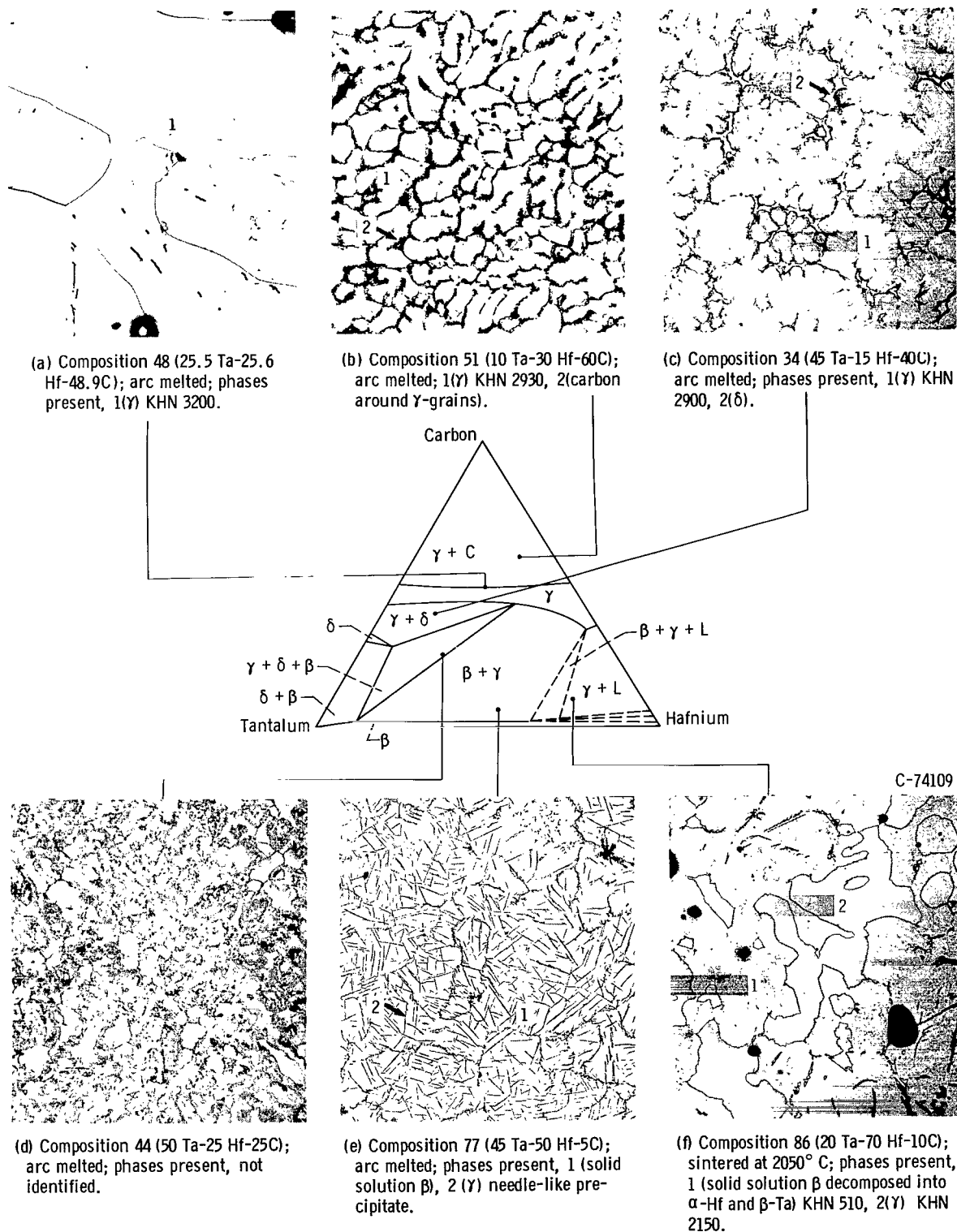
Figure 4(a), composition 48, is a typical microstructure of compositions in the region of the TaC-HfC pseudobinary system. With the exception of a few black areas, possibly due to porosity, impurities, or free carbon, only the  $\gamma$ -phase  $(\text{Ta,Hf})\text{C}_{1-x}$  (with nearly maximum carbon content) is present.

The structure shown in figure 4(b) is typical of the  $\gamma(\text{Ta,Hf})\text{C}_{1-x}$  + carbon phase field. Here completely carbon-saturated grains of  $\gamma$ -phase are found surrounded by carbon.

Composition 34, shown in figure 4(c), is typical of the  $\gamma(\text{Ta,Hf})\text{C}_{1-x}$  +  $\delta(\text{Ta,Hf})_2\text{C}_{1-x}$  phase field. The major component is the striated  $\gamma$ -phase. Similar striated structures have been observed in Ta-C binary compositions and reference 9 suggests these are the result of  $\text{Ta}_2\text{C}$  precipitation. The non-striated, intergranular component is the lower melting  $\delta$ -phase.

Composition 44, within the three-phase area, yields a quite indiscernible microstructure, as shown in figure 4(d). The light areas are probably





$\gamma$ -phase  $(\text{Ta,Hf})\text{C}_{1-x}$ . An x-ray diffraction pattern taken from the sample revealed the presence of three phases,  $\gamma(\text{Ta,Hf})\text{C}_{1-x}$ ,  $\delta(\text{Ta,Hf})_2\text{C}_{1-x}$ , and  $\beta(\text{Ta,Hf})$ .

The two-phase  $\gamma(\text{Ta,Hf})\text{C}_{1-x} + \beta(\text{Ta,Hf})$  equilibrium area is represented in figure 4(e). The matrix is mostly  $\beta$ -phase,  $(\text{Ta,Hf})$ , with a needle-like precipitate of  $\gamma$ -phase,  $(\text{Ta,Hf})\text{C}_{1-x}$ . Here one would expect to see an  $\alpha$ -hafnium phase as a result of the decomposition of  $\beta(\text{Ta,Hf})$  solid solution (at  $2050^\circ\text{C}$ ) on cooling. This was not the case, however, and the absence of  $\alpha$ -hafnium was also verified by the x-ray diffraction method.

The photomicrograph of composition 86 is shown in figure 4(f). The metallic phase, which was liquid at  $2050^\circ\text{C}$ , yielded, on cooling, a mixture of  $\alpha$ -Hf and  $\beta$ -Ta. The  $\gamma$ -phase,  $(\text{Ta,Hf})\text{C}_{1-x}$ , forms large grains of irregular shape surrounded by the fine-textured  $\alpha$ -Hf +  $\beta$ -Ta mixture. After heat treatment at  $2050^\circ\text{C}$  this specimen was deformed as a result of the presence of a liquid phase.

### Microhardness

Microhardness information from references 10 to 12 as well as present data are shown in figure 5. The Knoop hardness values for the  $\gamma$ -phase,  $(\text{Ta,Hf})\text{C}_{1-x}$ , vary from 1100 kilograms per square millimeter for carbon-deficient TaC to 3720 kilograms per square millimeter, when the hafnium content reaches about 11 atomic percent and the carbon is 48 atomic percent. Further increase in hafnium content, while approximately the same carbon content is maintained, causes a decrease in hardness. Completely carburized  $\gamma$ -phase compositions, in particular  $\text{TaC}_{1.0}$ , are significantly softer than carbon-deficient compositions. Figure 5 also shows that the hardness of the  $\beta$ -phase,  $(\text{Ta,Hf})$ , in the  $\gamma + \beta$  field appears to increase with increasing hafnium content; however, the metallic matrix formed on cooling the composition in the  $\gamma + \text{L}$  area is softer even though the hafnium content is greater than compositions in the  $\gamma + \beta$  field. The  $\gamma$ -phase  $(\text{Ta,Hf})\text{C}_{1-x}$  in the  $\gamma + \text{L}$  area is also softer than that in the  $\gamma + \beta$  region.

### DISCUSSION

On the basis of the previously described results, the phase boundaries shown in figure 2 were traced, and an isothermal section at  $2050^\circ\text{C}$  was constructed. The hafnium-rich corner of the diagram contains a liquid phase and the position of the phase boundaries were deduced primarily from the Ta-Hf and Hf-C binary systems and the observed deformation of compositions of high hafnium content due to liquid formation.

In general, the phase relations at  $2050^\circ\text{C}$  are similar to those at  $1850^\circ\text{C}$  except for the presence of the liquid phase. No phases other than those present in the binary systems were observed. The  $\zeta$ -phase sometimes found in the binary Ta-C system and shown as a dotted area in the ternary system at  $1850^\circ\text{C}$  (fig. 1) was not detected at  $2050^\circ\text{C}$ . The solubility of carbon in the  $\beta$ -phase is about 2 to 3 atomic percent. The solubility of carbon in tantalum at  $2050^\circ\text{C}$  is given as about 2.2 atomic percent in reference 13. The transformation of the  $\beta$ -phase,  $(\text{Ta,Hf})$  solid solution into  $\beta$ -Ta and  $\alpha$ -Hf at the



cooling rate used in this study occurs only at high hafnium contents.

The  $(\text{Ta,Hf})_2\text{C}_{1-x}$  phase does not accept more than about 8 atomic percent hafnium at  $2050^\circ\text{C}$ . This occurs at the expense of tantalum and is accompanied by an increase in lattice parameter from  $a_0 = 3.108$  angstroms,  $c_0 = 4.948$  angstroms for  $\text{Ta}_2\text{C}$  to  $a_0 = 3.120$  angstroms and  $c_0 = 4.970$  angstroms for hafnium-saturated  $\text{Ta}_2\text{C}$ .

There is complete solid solubility between  $\text{TaC}$  and  $\text{HfC}$ , and the carbon content in the  $\gamma$ -phase,  $(\text{Ta,Hf})\text{C}_{1-x}$ , may vary significantly. A hardness maximum appears to occur in the vicinity of 11 atomic percent hafnium, 41 atomic percent tantalum, and 48 atomic percent carbon (composition 30), which is near the compositions for which the highest melting point (ref. 1) and lowest vaporization rate (ref. 2) have been reported.

### CONCLUSIONS

An isothermal cross section of the Ta-Hf-C system at  $2050^\circ\text{C}$  was constructed from x-ray diffraction, chemical analysis, metallographic, and microhardness data. The complete solid solubility between  $\text{TaC}$  and  $\text{HfC}$  was verified. The lattice parameters of  $(\text{Ta,Hf})\text{C}_{1-x}$  solutions were determined. No phases other than those appearing in the three binary systems were observed. A liquid phase was found to be present in a large portion of the hafnium-rich corner. There is an exchange of hafnium for tantalum in the  $\delta(\text{Ta,Hf})_2\text{C}_{1-x}$  phase up to about 8 atomic percent. The lattice parameters increase correspondingly to  $a_0 = 3.120$  angstroms and  $c_0 = 4.970$  angstroms.

The  $\zeta$ -phase, sometimes found in the Ta-C system, was not observed in any of the compositions investigated at  $2050^\circ\text{C}$ . The limit of the  $\gamma(\text{Ta,Hf})\text{C}_{1-x} + \delta(\text{Ta,Hf})_2\text{C}_{1-x}$  area extends to about 38 atomic percent hafnium, which agrees with that at  $1850^\circ\text{C}$ . The solubility of carbon in the  $\beta(\text{Ta,Hf})$  solid solution is about 2 to 3 atomic percent.

Lewis Research Center,  
National Aeronautics and Space Administration,  
Cleveland, Ohio, January 26, 1965.

### REFERENCES

1. Agte, C.; and Alterthum, H.: Systems of High-Melting Carbides: Contributions to the Problem of Carbon Fusion. Z. tech. Physik, vol. 11, 1930, pp. 182-191.
2. Deadmore, Daniel L.: Vaporization of Tantalum-Carbide - Hafnium-Carbide Solid Solutions at  $2500^\circ$  to  $3000^\circ\text{K}$ . NASA TN D-2512, 1964.
3. Rudy, E.; and Nowotny, H.: Investigation of the Hafnium-Tantalum-Carbon System. Monatsh. für Chem., vol. 94, no. 3, 1963, pp. 507-517.

4. Storms, E. K.: A Critical Review of Refractories. Pt. I. Selected Properties of Group 4a, 5a, and 6a Carbides. Rept. No. LAMS-2674, Los Alamos Sci. Lab., Feb. 1, 1962, p. 50.
5. Benesovsky, F.; and Rudy, E.: The Constitution of the Zirconium-Carbon and Hafnium-Carbon Systems. Planseeber. Pulvermet, vol. 8, 1960, pp. 66-71.
6. Kato, H.; Armantrout, C. E.; and Deardorff, D. K.: Hafnium Alloys. USBM-U-783, Quart. Met. Prog. Rept. No. 9, Oct. 1-Dec. 31, 1960, Albany Met. Res. Center, Dec. 1960, pp. 15-16.
7. Bowman, Allen L.: The Variation of Lattice Parameter with Carbon Content of Tantalum Carbide. J. Phys. Chem., vol. 65, no. 9, Sept. 1961, pp. 1596-1598.
8. Bittner, H.; and Goretzki, H.: Magnetic Researches on the Carbides TiC, ZrC, HfC, VC, NbC, and TaC. Monatsh. für Chem., vol. 93, 1962, pp. 1000-1004.
9. Santoro, G.; and Probst, H. B.: An Exploration of Microstructures in the Tantalum-Carbon System. Advances in X-Ray Analysis, Vol. 7, W. M. Mueller, G. Mallett, and M. Fay, eds., Plenum Press, 1963, pp. 126-135.
10. Adams, R. P.; and Beall, R. A.: Preparation and Evaluation of Fused Hafnium Carbide. Rept. No. BM-RI-6304, 1963. Bur. of Mines.
11. Santoro, Gilbert: Variation of Some Properties of Tantalum Carbide with Carbon Content. Trans. Met. Soc. AIME, vol. 227, Dec. 1963, pp. 1361-1368.
12. Litton, F. B.: Preparation and Some Properties of Hafnium Metal. J. Electrochem. Soc., vol. 98, 1951, pp. 488-494.
13. Ogden, H. R.; Schmidt, F. F.; and Bartlett, E. S.: The Solubility of Carbon in Tantalum. Trans. Met. Soc. AIME, vol. 227, Dec. 1963, pp. 1458-1460.

TABLE I. - CHEMICAL ANALYSIS OF  
STARTING MATERIALS

Tantalum hydride	
Element	Weight percent
H	0.49
O	.072
N	.031
Si,W	0.005 - 0.05
Fe,Zr	0.01 - 0.10
Ti,Cu,Ni,V,Mn,Nb, Ca,Mg,Pb,Ba,K	<0.01
All other elements	All other elements not detected
Hafnium hydride	
H	1.1
Zr	1.6
O	.02
N	.003
Fe	.025
C	.015
B,U,Cd	<.001
Al,Mo,Si,W,Cr,Pb, Ni,Na,Co,Mg,Sn, V,Ca,Cu,Mn,Ti }	0.001 - 0.01

TABLE II. - COMPOSITION, PREPARATION, AND ROOM TEMPERATURE X-RAY DIFFRACTION DATA

Sample number	Composition, atomic percent			Method of preparation	Number of phases detected by room temperature x-ray diffraction	Phases present by room-temperature x-ray diffraction and lattice parameters <sup>a</sup>						Sample number	Composition, atomic percent			Method of preparation	Number of phases detected by room temperature x-ray diffraction	Phases present by room-temperature x-ray diffraction and lattice parameters <sup>a</sup>							
	Tantalum	Hafnium	Carbon			$\beta(\text{Ta,Hf})$		$\alpha(\text{Hf,Ta})$		$\delta(\text{Ta,Hf})_{2\text{C}_{1-x}}$			$\gamma(\text{Ta,Hf})\text{C}_{1-x}$	Tantalum	Hafnium			Carbon	$\beta(\text{Ta,Hf})$		$\alpha(\text{Hf,Ta})$		$\delta(\text{Ta,Hf})_{2\text{C}_{1-x}}$		$\gamma(\text{Ta,Hf})\text{C}_{1-x}$
						Body centered cubic	Hexagonal	Hexagonal	Face centered cubic	Body centered cubic	Hexagonal								Hexagonal	Face centered cubic	Body centered cubic	Hexagonal	Hexagonal	Face centered cubic	
						$a_0$	$a_0$	$c_0$	$a_0$	$c_0$	$a_0$							$a_0$	$a_0$	$c_0$	$a_0$	$c_0$	$a_0$		
1	80	0	20	Sintered	2	3.306	N.D.	N.D.	3.103	4.936	N.D.	51	10	50	60	Arc melted	2	N.D.	N.D.	N.D.	N.D.	N.D.	4.578 + Carbon		
2	71	29		Sintered	2	N.L.	N.L.		3.103	4.948	N.D.	52	50.5	17.5	32	Sintered	3	N.L.	N.D.	N.D.	N.D.	3.128	4.978	4.550	
3	64	36		Arc-melted	2	N.D.	N.D.		3.106	4.948	N.L.	53	47	17	36		2	N.D.	N.D.	N.D.	N.D.	3.111	4.946	4.532	
4	52	48		Hot pressed	1	N.D.	N.D.		N.D.	N.D.	4.455	54	30	50	40		2	N.D.	N.D.	N.D.	N.D.	3.127	4.981	4.527	
5	51	49		Sintered	1	N.D.	N.D.		N.D.	N.D.	4.455	55	52.5	27.5	20		2	3.321	N.D.	N.D.	N.D.	N.D.	4.552		
6	93.5	.5	6		2	3.309	N.L.	N.L.	N.D.	N.D.		56	42	23	35		3	N.L.	N.D.	N.D.	N.D.	3.120	4.979	4.544	
7	89.8	.2	10		2	3.308	N.L.	N.L.		3.113	4.968	57	29.8	34.7	35.5	Arc melted	2	N.D.	N.D.	N.D.	N.D.	N.L.	N.L.	4.511	
8	78.5	2.7	18.8			N.L.	N.L.		3.111	4.955		58	31	28	41	Hot pressed	2					3.121	4.969	4.546	
9	70.1	1.1	29.8			N.L.	N.L.		3.109	4.942		59	19.6	36.9	43.5	Arc melted	1					N.D.	N.D.	4.550	
10	60.6	1.5	37.9			N.D.	N.D.		3.106	4.942	4.414	60	12.6	37.8	49.5	Hot pressed	1					N.D.	N.D.	4.590	
11	55.6	1.7	42.7			N.D.	N.D.		N.L.	N.L.	4.419	61	53.2	33.4	1.4	Sintered	1	3.363	N.D.	N.D.	N.D.	N.D.	N.D.		
12	60	3	37			N.D.	N.D.		3.110	4.949	4.451	62	30	40	30	Sintered	2	N.D.	N.D.	N.D.	N.D.	N.L.	N.L.	4.585	
13	73	5	22			3.309	N.D.		3.116	4.953	N.D.	63	34.3	31.5	34	Sintered	3	N.L.	N.D.	N.D.	N.D.	N.L.	N.L.	4.543	
14	69	4	27			3.312	N.D.		3.122	4.971	N.D.	64	10	42.6	47.4	Arc melted	1	N.D.	N.D.	N.D.	N.D.	N.D.	N.D.	4.593	
15	65.9	5.9	28.2			N.L.	N.L.		3.114	4.950	N.D.	65	35	35	30	Sintered	2	3.324	N.D.	N.D.	N.D.	N.D.	N.D.	4.551	
16	64	5.2	30.8			N.D.	N.D.		3.111	4.943	N.L.	66	34	24	32			N.L.	N.D.	N.D.	N.D.	N.D.	N.D.	4.553	
17	64.5	3.4	32.1			N.D.	N.D.		3.107	4.946	4.437	67	29	40	31			3.356	N.D.	N.D.	N.D.	N.D.	N.D.	4.584	
18	60.7	5.4	33.9			N.D.	N.D.		3.109	4.955	N.L.	68	33.5	33.5	21			N.L.	N.D.	N.D.	N.D.	N.D.	N.D.	4.595	
19	52.5	7.5	40			N.L.	N.L.		N.L.	N.L.	4.418	69	34	35	24			3.373	N.D.	N.D.	N.D.	N.D.	N.D.	4.594	
20	87.9	7.8	4.3			3.316	N.D.		3.125	4.971	N.D.	70	20.4	45.1	34.5	Arc melted		N.L.	N.D.	N.D.	N.D.	N.D.	N.D.	4.545	
21	81.1	9.4	9.5			N.L.	N.L.		3.137	5.003	N.D.	71	52.3	42	5.7	Sintered		3.367	N.D.	N.D.	N.D.	N.D.	N.D.	N.L.	
22	64.1	7.6	28.1			N.L.	N.L.		3.115	4.954	N.D.	72	56	36	0	Sintered		3.371	N.D.	N.D.	N.D.	N.D.	N.D.	4.590	
23	75	9.0	29.1			N.D.	N.D.		3.114	4.942	N.L.	73	34	45	18	Sintered		3.372	N.D.	N.D.	N.D.	N.D.	N.D.	4.596	
24	61.3	7.2	31.5			N.D.	N.D.		3.101	4.940	N.L.	74	15	45	37	Arc melted		N.L.	N.D.	N.D.	N.D.	N.D.	N.D.	4.556	
25	57.7	6.6	35.7			N.D.	N.D.		3.106	4.945	4.444	75	36.5	33.5	24	Sintered		3.364	N.D.	N.D.	N.D.	N.D.	N.D.	4.588	
26	54.5	10.5	35			N.D.	N.D.		3.121	4.971	4.504	76	5	48	47	Arc melted	1	N.D.	N.D.	N.D.	N.D.	N.D.	N.D.	4.595	
27	65	10	25			3.321	N.D.		3.129	4.993	4.558	77	45	50	5	Sintered	2	3.403	N.D.	N.D.	N.D.	N.D.	N.D.	4.611	
28	30	10	60	Arc melted	2	N.D.	N.D.		N.D.	N.D.	4.469 + Carbon	78	24	43	27			3.388	N.D.	N.D.	N.D.	N.D.	N.D.	4.602	
29	49.3	10	40.7	Arc melted	2	N.L.	N.L.		N.L.	N.L.	4.442	79	24.5	43.5	26			N.L.	N.D.	N.D.	N.D.	N.D.	N.D.	4.602	
30	41	11	48	Hot pressed	1	N.D.	N.D.		N.D.	N.D.	4.482	80	17.5	50.5	32			N.L.	N.D.	N.D.	N.D.	N.D.	N.D.	4.581	
31	46.7	9.9	43.4	Arc melted	1	N.D.	N.D.		N.D.	N.D.	4.455	81	6	57	37			N.D.	N.D.	N.D.	N.D.	N.D.	N.D.	4.583	
32	55	10.3	34.7	Sintered	2	3.125	4.981	4.534	3.125	4.981	4.534	82	11.5	46.5	42			N.D.	N.D.	N.D.	N.D.	N.D.	N.D.	4.585	
33	50	15	35			3.120	4.963	4.500	3.120	4.963	4.500	83	20	60	20			N.L.	N.D.	N.D.	N.D.	N.D.	N.D.	4.598	
34	45	15	40			3.112	4.954	4.504	3.112	4.954	4.504	84	40	50	10			3.363	N.D.	N.D.	N.D.	N.D.	N.D.	4.602	
35	74	15.2	10.8			3.319	N.L.	N.L.	N.L.	N.L.	4.556	85	7.5	67.5	25			N.L.	N.D.	N.D.	N.D.	N.D.	N.D.	4.609	
36	80	15	5	Arc melted	2	3.354	N.D.	N.D.	N.L.	N.L.		86	20	70	10			N.L.	N.D.	N.D.	N.D.	N.D.	N.D.	4.595	
37	64	15.6	20.4	Sintered	1	3.324	N.L.	N.L.	N.L.	N.L.	4.547	87	26	66	8			3.370	N.D.	N.D.	N.D.	N.D.	N.D.	4.602	
38	57	15	28			N.L.	N.L.		3.132	4.994	4.543	88	8.5	78.5	13			N.D.	N.D.	N.D.	N.D.	N.D.	N.D.	4.608	
39	56	14	30			N.L.	N.L.		3.125	4.985	4.553	89	5.7	63.8	27.5			3.222	N.D.	N.D.	N.D.	N.D.	N.D.	4.626	
40	50	17	33			N.L.	N.L.		3.131	4.986	4.557	90	0	50.4	49.6	Hot pressed	1		N.D.	N.D.	N.D.	N.D.	N.D.	4.640	
41	75.7	22.9	1.5			3.352	N.D.	N.D.	N.D.	N.D.		91	0	53.8	46.2	Sintered								4.642	
42	61	20	19			3.310	N.L.	N.L.	N.L.	N.L.	4.556	92	0	58	42									4.635	
43	39.4	22	38.6	Arc melted	2	N.D.	N.D.		N.L.	N.L.	4.471	93	0	53	41			3.329	N.D.	N.D.	N.D.	N.D.	N.D.	4.627	
44	50	25	25	Sintered	3	3.321	N.L.	N.L.	N.L.	N.L.	4.546	94	5.6	14	0									N.D.	
45	64	26	10	Sintered	2	3.346	N.D.	N.D.	N.D.	N.D.	4.585	95	5.0	20	0	Arc melted		3.334	N.D.	N.D.	N.D.	N.D.	N.D.	N.D.	
46	41.5	21.5	37	Sintered	2	N.D.	N.D.		3.121	4.955	4.510														
47	28.5	25.1	46.4	Arc melted	1	N.D.	N.D.		N.D.	N.D.	4.526														
48	25.5	25.6	48.9	Hot pressed	1						4.552														
49	24.7	27.7	47.6	Arc melted	1						4.535														
50	67.4	26.7	5.9	Sintered	2	3.361					N.L.														

<sup>a</sup>All lattice parameters are given in angstrom units, with a standard deviation of  $\pm 0.005$ .<sup>b</sup>Phase was not detected by x-ray diffraction.<sup>c</sup>Phase was detected, but because too few lines were present for accurate calculation of the lattice parameter, none is given.

2/22/85  
2

*"The aeronautical and space activities of the United States shall be conducted so as to contribute . . . to the expansion of human knowledge of phenomena in the atmosphere and space. The Administration shall provide for the widest practicable and appropriate dissemination of information concerning its activities and the results thereof."*

—NATIONAL AERONAUTICS AND SPACE ACT OF 1958

## NASA SCIENTIFIC AND TECHNICAL PUBLICATIONS

**TECHNICAL REPORTS:** Scientific and technical information considered important, complete, and a lasting contribution to existing knowledge.

**TECHNICAL NOTES:** Information less broad in scope but nevertheless of importance as a contribution to existing knowledge.

**TECHNICAL MEMORANDUMS:** Information receiving limited distribution because of preliminary data, security classification, or other reasons.

**CONTRACTOR REPORTS:** Technical information generated in connection with a NASA contract or grant and released under NASA auspices.

**TECHNICAL TRANSLATIONS:** Information published in a foreign language considered to merit NASA distribution in English.

**TECHNICAL REPRINTS:** Information derived from NASA activities and initially published in the form of journal articles.

**SPECIAL PUBLICATIONS:** Information derived from or of value to NASA activities but not necessarily reporting the results of individual NASA-programmed scientific efforts. Publications include conference proceedings, monographs, data compilations, handbooks, sourcebooks, and special bibliographies.

*Details on the availability of these publications may be obtained from:*

SCIENTIFIC AND TECHNICAL INFORMATION DIVISION  
NATIONAL AERONAUTICS AND SPACE ADMINISTRATION  
Washington, D.C. 20546